Quantum Machine Intelligence (2023) 5:2
https://doi.org/10.1007/s42484-022-00089-7

RESEARCH ARTICLE

Quantum image representation: a review

Marina Lisnichenko[1] · **Stanislav Protasov**[1]

Received: 2 September 2022 / Accepted: 12 November 2022 / Published online: 26 December 2022

Abstract
Quantum programs allow to process multiple bits of information at the same time, which is useful in multidimensional data handling. Images are an example of such multidimensional data. Our work reviews 14 quantum image encoding works and compares implementations of 8 of them by 3 metrics: number of utilized qubits, quantum circuit depth, and quantum volume. Our work includes a practical comparison of $2^n \times 2^n$ images encoding, where n varies from 1 up to 8. We observed that Qubit Lattice approach shows the minimum circuit depth as well as quantum volume, Flexible Representation of Quantum Images (FRQI) utilizes the minimum number of qubits. If to talk about variety of processing techniques, FRQI and Novel Enhanced Quantum Representation (NEQR) representations are the most fruitful. As far as quantum computers are limited in qubit number, we concluded that almost all approaches except Qubit Lattice are promising for the near future of quantum image representation and processing. From the point of view of the quantum depth, discrete methods showed the most appropriate result.

Keywords Quantum images · Complexity · Quantum algorithms · Quantum image processing

1 Introduction

Quantum computation is a rapidly developing field. In 2021 private capital investments in quantum computations exceeded $3B (Leprince-Ringuet 2021). Due to the quantum parallelism the information processing is performed potentially faster. Acceleration of the calculations through parallelism is highly relevant to multidimensional data, including images. In the quantum programs, images are usually represented in the same way as in classical machines — with pixel coordinates and pixel intensities, but amplitude and phase encodings use different physical parameters for these values. In this work, we compare 14 ways of image encoding including methods: with quantum state amplitudes — amplitude-angular (continuous), qubit binary — amplitude-state (discrete), mixed, and phase image representations. We implemented 8 core representation techniques (other methods are derived or equivalent to the implemented and share their characteristics) for the practical comparison[1]. Our survey covers the following quantum image representation methods:

- qubit lattice (Venegas-Andraca and Bose 2003);
- real ket (Latorre 2005);
- flexible representation of quantum images — FRQI (Le et al. 2011);
- multichannel representation for images — MCRQI (Sun et al. 2011);
- novel enhanced quantum representation of digital images — NEQR (Zhang et al. 2013);
- quantum states for M colors and quantum states for N coordinates — QSMC and QSNC (Li et al. 2013);
- a simple quantum representation — SQR (Yuan et al. 2014);
- normal arbitrary quantum superposition state — NAQSS (Li et al. 2014);
- generalized quantum image representation — GQIR (Jiang et al. 2015);
- quantum representation of multi-wavelength images — QRMW (Şahin and Yilmaz 2018);
- quantum image representation based on bitplanes — BRQI (Li et al. 2018);

✉ Marina Lisnichenko
m.lisnichenko@innopolis.university

Stanislav Protasov
s.protasov@innopolis.ru

[1] MLKR Laboratory, Innopolis University, Universitetskaya, Innopolis, 420500, Tatarstan Republic, Russia

[1] github.com/UralmashFox/QPI

- order-encoded quantum image model — OQIM (Xu et al. 2019);
- quantum representation of indexed images and its applications — QIIR (Wang et al. 2020);
- Fourier transform qubit representation — FTQR (Grigoryan and Agaian 2020).

The review contains the information about quantum image representation methods and applicable image processing techniques. To compare the methods, we use 3 parameters:

- *number of utilized qubits* — each existing computer is limited in number of qubits and this number defines the possibility of algorithm execution;
- *circuit depth* — length of the longest quantum gate path from the zero-state to the end of the encoding procedure. The bigger the depth is, the more errors affect on the output result quality. This metric is an analogy of the classical time complexity;
- *quantum volume* — squared minimum between the circuit depth and number of qubits. This metric varies for different quantum machines, and depends on the base gates. Quantum volume is an integral metric which allows to evaluate a computing capability with a single quantity.

In Section 3 we sum the observed information and make a statement about future work.

2 Quantum image representation (QIR) techniques

We identified four major ways of quantum image representation: **continuous amplitude** representation, where pixel intensity is encoded with quantum state amplitude p, corresponding to observation probability p^2, **amplitude with binary intensity** representation (discrete), **mixed**, and **phase intensity** representation. Figure 1 shows the suggested classification.

Continuous representation allows to use a single qubit for intensity or coordinate encoding. This is the main advantage of the methods. Multiple measurements are required to estimate the pixel intensity with high precision.

In the discrete intensity representation, oppositely, each state corresponds to separate intensity or coordinate bit-value. Measurement result contains accurate data expansion of a single pixel data.

Mixed representations either store pixel coordinates discretely or do not encode coordinate.

Phase encoding uses continuous representation, but in an XY Bloch sphere projection plane.

In the following subsections, we describe each approach separately.

2.1 Mixed representation

The chapter describes quantum image representation algorithms based on both discrete and continuous methods. It is common for mixed methods where continuous encoding is used for the pixel intensity and the pixel location is represented discretely. We also include Qubit Lattice and SQR algorithms; however, these methods do not have a specific coordinate encoding procedure.

2.1.1 Qubit lattice

Venegas-Andraca and Bose (2003) did a major preparatory work in the quantum image representation and processing. The paper describes the basic quantum definitions and measured results interpretation. Proposed image representation is naïve and consists of literally copying the classical representation into quantum. Authors suggest to use R_y rotation gate to set each pixel's intensity. Therefore, the number of utilized qubits is 2^{2n} where $2^n \times 2^n$ is an image size. Figure 2b shows an example of encoding the image with pixel intensities $\{0, 125, 200, 255\}$.

Coordinate qubits absence and quantum circuit simplicity are the strong sides of the encoding method. Due to simplicity, authors of quantum convolutional neural networks papers actively utilize this representation method (or modified) even if it is not evidently claimed (Oh et al. 2020; Cong et al. 2019; Yang et al. 2021). At the same time, classical image processing based on Qubit Lattice did not spread. Qubit Lattice does not use such quantum features as entanglement and superposition. Thus, the approach has strong negative sides such as big number of used qubits and small number of known processing methods. However, for the

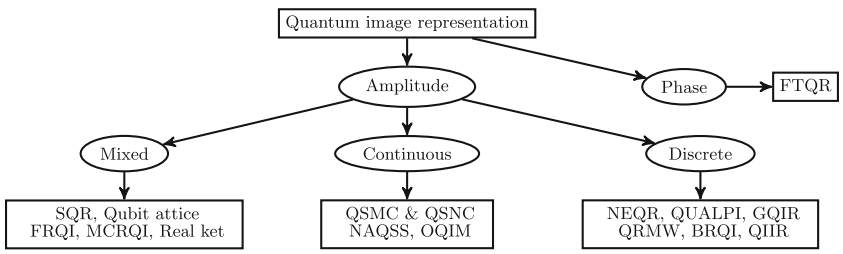

Fig. 1 Quantum image representation (QIR) classification

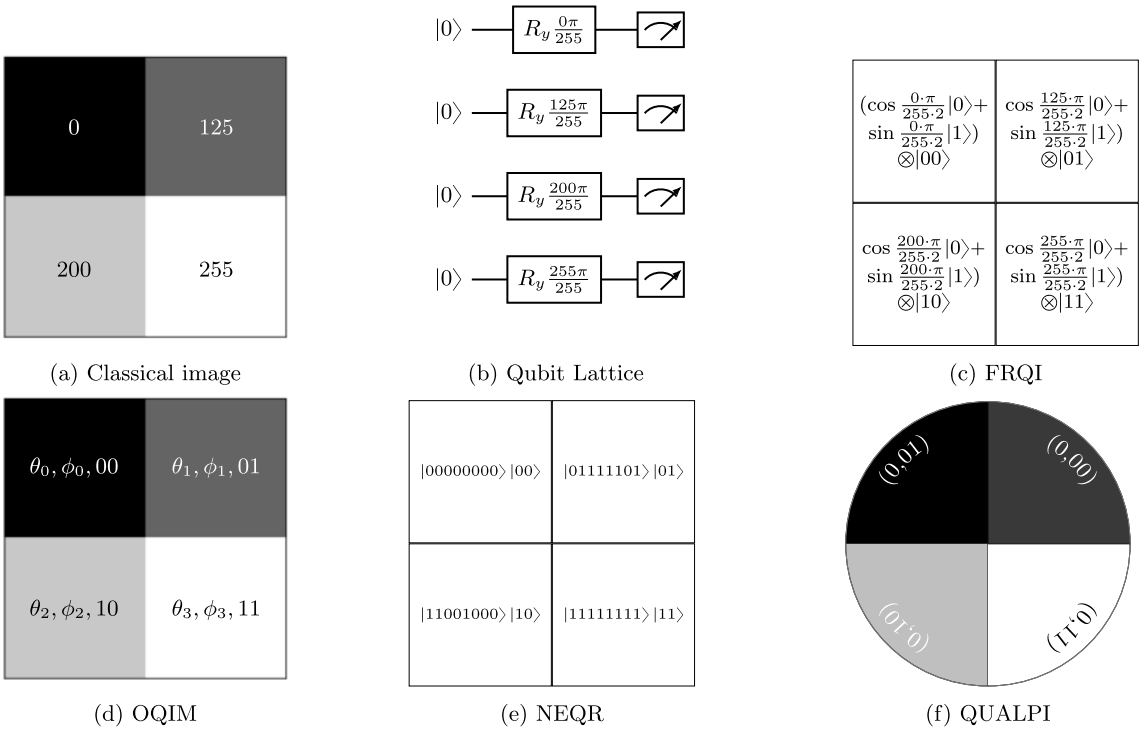

Fig. 2 (a) Classical image and (b–f) quantum image representations

sake of justice, it is the first formulation of quantum image storing.

2.1.2 FRQI

Authors (Le et al. 2011) use the continuous amplitude encoding with intensity-to-amplitude representation.

$$| I(\alpha)\rangle = \frac{1}{2^n} \sum_{i=0}^{2^{2n}-1} (cos\alpha_i \mid 0\rangle + sin\alpha_i \mid 1\rangle) \otimes \mid i\rangle \qquad (1)$$

where $| I(\alpha)\rangle$ is a quantum image representation, α is a parameter responsible for intensity and equal to a half of R_y rotation angle, $| i\rangle$ represents the pixel coordinate binary expansion. The greater α is, the closer pixel intensity to the maximum. Therefore, the precision of the intensity estimation depends on the number of circuit executions.

Figure 2c shows the image with pixel intensities $\{0, 125, 200, 255\}$. The image representation code is available in our repository.

The FRQI implies a huge number of processing algorithms. For example, the paper presents processing algorithms that affect intensity, coordinate, or both intensity and coordinate. The first processing group changes all the pixel intensities, the second group changes intensity at some locations, the last group "targets information about both color and position as in Fourier transform". Moreover, multichannel expansion (Yan and Venegas-Andraca 2020), image compression, line detection (Le et al. 2011), binarization, histogram computing, histogram equalization (Caraiman and Manta 2012), global and local translation designs (Zhou et al. 2017) are also available for FRQI. The image representation technique maintains comprehensive processing such as information hiding (Thenmozhi et al. 2021), Richardson-Lucy image restoration (Ma et al. 2020), multilevel segmentation (Tariq Jamal et al. 2021), hybrid images creating (Farina 2021). Additionally, FRQI helps to find correlation property of multipartite quantum image (Sanchez et al. 2019), implement image fusion (Liu and Xiao 2019), encrypt images via algorithm based on Arnold scrambling and wavelet transforms (Hu et al. 2020).

At the same time, FRQI has the following drawbacks:

- FRQI do not make possible to encode intensity in one-by-one mode. Thus, it ignores the QPU data loading interface (Mastriani 2020).
- due to the single intensity qubit "some digital image-processing operations for example certain complex color operations", are impossible (such as "partial color operations and statistical color operations") (Zhang et al. 2013).
- circuit depth is $O(2^{4n})$ for $2^n \times 2^n$ image (Zhang et al. 2013).

FRQI is beneficial for the applications with limited qubit number and does not demand high intensity precision. FRQI supports broad spectrum of quantum image processing

techniques useful for basic image processing. However, the continuous intensity representation approach may limit such processing algorithms as edge detection and texture features.

2.1.3 MCRQI

The authors of Sun et al. (2011) apply FRQI (Section 2.1.2) approach to the $RGB\alpha$ images, where α is a transparency channel. The difference is in the number of qubits used to encode an intensity. Authors represent the multichannel image as follows:

$$|\, I(\theta)\rangle = \frac{1}{2^n} \sum_{i=0}^{2^{2n}-1} |\, c^i_{RGB\alpha}\rangle \otimes |\, i\rangle \tag{2}$$

where $|\, c^i_{RGB\alpha}\rangle$ is a color state and equals to:

$$|\, c^i_{RGB\alpha}\rangle = \frac{1}{2}\left(\begin{bmatrix} \cos\theta_{Ri} \,|\, 0\rangle \\ \sin\theta_{Ri} \,|\, 1\rangle \end{bmatrix} \otimes |\, 00\rangle + \begin{bmatrix} \cos\theta_{Gi} \,|\, 0\rangle \\ \sin\theta_{Gi} \,|\, 1\rangle \end{bmatrix} \otimes |\, 01\rangle + \begin{bmatrix} \cos\theta_{Bi} \,|\, 0\rangle \\ \sin\theta_{Bi} \,|\, 1\rangle \end{bmatrix} \otimes |\, 10\rangle + \begin{bmatrix} \cos\theta_{\alpha i} \,|\, 0\rangle \\ \sin\theta_{\alpha i} \,|\, 1\rangle \end{bmatrix} \otimes |\, 11\rangle \right). \tag{3}$$

Multichannel representation encodes intensities $\in [0, 255]$ with angles $\theta_{Ri}, \theta_{Gi}, \theta_{Bi}, \theta_{\alpha i} \in [0, \frac{\pi}{2}]$ via uniform scaling. As far as image has several channels, authors say about applicability of the one-channel operations for each of them. Authors (Yan et al. 2018) developed a chromatic framework for quantum movies and provided frame-to-frame and color of interest operations, sub-block swapping. Yan et al. described audio-visual synchronization in quantum movies using MCRQI (Yan et al. 2018). Sun et al. proposed channel of interest realization, channel-swapping and α blending operations (Sun et al. 2014). Hu et at. all proposed image encryption based on FRQI modification (Hu et al. 2020). The MCRQI has the same pros and cons as the FRQI. Additionally, to get access to each color layer channels *r, g, b* has to be measured separately.

2.1.4 SQR

The authors (Yuan et al. 2014) combine Qubit Lattice image representation with normalized pixels and NEQR (see Section 2.3.1) approach of max and minimum pixel values. Instead of pixel intensity authors use "energy" term to show the relation to the infrared images. Their paper describes the Qubit Lattice approach (Venegas-Andraca and Bose 2003) with modifications. Authors of the Qubit Lattice converted intensities directly into angles, while in SQR intensities go through a normalization step first. Suppose, E_{ij} is an energy value detected at the position i, j, E_m minimum energy value, E_M maximum energy value. The normalized energy value is $\tilde{E_{ij}} = \frac{E_{ij} - E_m}{E_M - E_m}$. $\tilde{E_{ij}}$ determines R_y rotation angle via the following expression:

$$\theta_{ij} = 2 \arcsin \tilde{E_{ij}} \tag{4}$$

To encode complete image information, 10 qubits store E_M and E_m energy values. Totally, to encode an image of size $2^n \times 2^n$ algorithm needs $2^n \times 2^n + 10$ qubits.

Authors provide clear explanation of how to convert energy into quantum representation and why is it so intuitive. Due to narrow representation specification, the SQR did not become widespread in terms of processing. Paper describes global and local operations, "retrieval of marked information" (kind of segmentation). However, the approach is still "heavy" in qubits.

2.1.5 Real Ket

Latorre (2005) attempted to separate a pixel's coordinates and intensity into quadrants. The first step of the encoding is to split image into 4 parts (upper-left, upper-right, lower-left, and lower-right). Next, the same step (splitting) repeats until each block contains a quad of pixels. A pair of qubits describes the grid-square pixel coordinate and additional qubit's amplitude holds intensity. This method, as well as FRQI, intensively uses multicontrol R_y gated (Fig. 3a), but Real Ket does not have a dedicated intensity qubit. In theorem 8 authors of Shende et al. (2006) proved that decomposition of one such k-qubit controlled gate requires 2^k CNOT gates.

Overall, the algorithm requires $2n + 1$ qubits, where $2^n \times 2^n$ is an image size. The final state equation is the following:

$$|\, \Psi_{2^n \times 2^n}\rangle = \sum_{i_1,\ldots,i_n=1,\ldots,4} c_{i_n,\ldots,i_1} \,|\, i_n, \ldots, i_1\rangle. \tag{5}$$

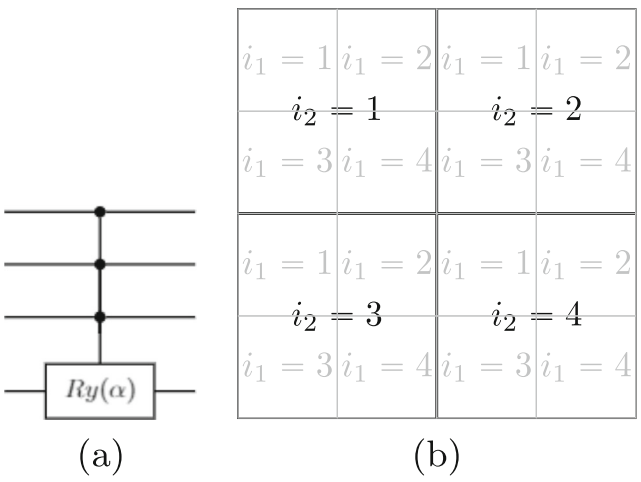

Fig. 3 (a) Multicontrol Ry gate (gate consists of 3 control qubits that rotate the last one — target — qubit for an angle α) and (b) Real Ket coordinate estimation

where $|\ \Psi\rangle$ is a quantum image, c_i pixel intensity, i_n is a representation of the pixel's location corner in the 4×4 grid. Figure 3b gives graphical pixels' coordinates representation for the 4×4 image.

Authors of the paper describe the image compression algorithm based on Fourier transform. Ma et al. proposed quantum Radon transform based on Real Ket encoding (Ma et al. 2021). The similar image representation is used for low-rank tensor completion (Ding et al. 2019).

2.2 Pure continuous representation

Representation algorithms of the current chapter utilize only continuous amplitude encoding for both pixel intensity and coordinates.

2.2.1 QSMC and QSNC

Suppose the image consists of m different pixel intensities taken from M possible (if an image is an 8-bit gray-scaled, $M = 256$), and contains $N = 2^n \times 2^n$ pixels. The authors (Li et al. 2013) split image representation into 3 parts: quantum register for m colors (QSMC), quantum register for N coordinates (QSNC), and image storing. Authors provide the following intensity representation algorithm, which we reproduced in our repository.

If $|\ w_i\rangle$ is a pixel intensity representation and $|\ u_i\rangle$ is a pixel coordinate representation, then full pixel representation is $|\ \psi_i\rangle = |\ w_i\rangle \otimes |\ u_i\rangle$.

The paper proves the reliability of the method from the mathematical prospects. Moreover, the authors provide a quantum image compression algorithm and image segmentation based on extended Grover search (Grover 1997). The method was not broadly utilized in quantum image processing and we could not find any publications based on it.

The main weakness of the method is the continuous approach to coordinate representation. When the number of pixels becomes bigger, even a small shift in probabilities affects the outcome. For example, IonQ QPU's R_y gate precision is $10^{-3}\pi$ radians (IonQ 2021), which makes impossible to encode coordinates of image larger than 512×512. In this case the coordinate encoding error becomes significant and coordinate estimation precision decreases.

2.2.2 OQIM

The authors (Xu et al. 2019) provide a way to store classical images by intensity sorting. Firstly, authors map the ordered pixel intensities present in the image to numbers. Then the continuous representation defines pixel color and coordinate (θ and ϕ respectively). Figure 2d provides an example of the 2×2.

The authors' idea is to utilize a single qubit for both intensity and coordinate. An additional qubit controls the mode of representation (coordinate or intensity). Thus, for the image represented in Fig. 2a the following equation holds:

$$
\begin{aligned}
|\ I\rangle = \frac{1}{2^{3/2}}\Big[& \\
&((\cos\theta_0\ |\ 0\rangle + \sin\theta_0\ |\ 1\rangle)\ |\ 0\rangle + (\cos\phi_0\ |\ 0\rangle + \sin\phi_0\ |\ 1\rangle)\ |\ 1\rangle)\otimes |\ 00\rangle + \\
&((\cos\theta_1\ |\ 0\rangle + \sin\theta_1\ |\ 1\rangle)\ |\ 0\rangle + (\cos\phi_1\ |\ 0\rangle + \sin\phi_1\ |\ 1\rangle)\ |\ 1\rangle)\otimes |\ 01\rangle + \\
&((\cos\theta_2\ |\ 0\rangle + \sin\theta_2\ |\ 1\rangle)\ |\ 0\rangle + (\cos\phi_2\ |\ 0\rangle + \sin\phi_2\ |\ 1\rangle)\ |\ 1\rangle)\otimes |\ 10\rangle + \\
&((\cos\theta_3\ |\ 0\rangle + \sin\theta_3\ |\ 1\rangle)\ |\ 0\rangle + (\cos\phi_3\ |\ 0\rangle + \sin\phi_3\ |\ 1\rangle)\ |\ 1\rangle)\otimes |\ 11\rangle\Big] \quad (6)
\end{aligned}
$$

Authors propose the histogram specification process that allows to shift the image histogram. Authors provide "image comparison between two images and multiple images..., the parallel quantum searching" (Guanlei et al. 2020). Paper also covers the multidimensional OQIM case. Basic algorithm implementation is available in our repository.

2.2.3 NAQSS

Authors' encoding approach (Li et al. 2014) is similar to the QSMC and QSNC (Section 2.2.1). Encoding starts with color representation. If $color_i$ represents the i^{th} pixel color, then colors $\{color_1, color_2, ..., color_M\}$ — a set of all possible colors for the image. Therefore, rotation angle $\phi_i = \frac{\pi(i-1)}{2(M-1)}$ defines i^{th} state rotation angle. For the RGB image, each color value is $i = R \times 256 \times 256 + G \times 256 + B + 1$ what takes range from $color_1 = (0, 0, 0)$ to $color_{16777216} = (255, 255, 255)$.

The coordinate representation is the following. Suppose data has k dimensions (for flat image we assume $k = 2$). Then, each pixel sets in the following state:

$$
|\ \psi_\phi\rangle = \sum_{i=0}^{2^n-1} a_i\ |\ v_1\rangle\ |\ v_2\rangle ...\ |\ v_k\rangle \quad (7)
$$

where $i = i_1...i_j i_{j+1}...i_l...i_m...i_n$ is a binary expansion of the coordinate $v_1 = i_1..i_j$, $v_2 = i_{j+1}...i_l$ and $v_k = i_m...i_n$ are the expansions of each coordinate separately.

The approach bases on a normalized intensity representation:

$$
\theta = \frac{a_i}{\sqrt{\sum_{y=0}^{2^n-1} a_y^2}}, \quad (8)
$$

where a_i is an intensity of current pixel i and $\sum_{i=0}^{2^n-1} \theta_i^2 = 1$.

Authors suggest to use image cropping and extend circuit by 1 qubit. The equation explains the cropped quantum image:

$$| \Psi\rangle = \sum_{i=0}^{2^n-1} \theta_i \mid v_1\rangle \mid v_2\rangle ... \mid v_k\rangle \mid \chi_i\rangle \tag{9}$$

where $\mid \chi_i\rangle = cos\gamma_i \mid 0\rangle + sin\gamma_i \mid 1\rangle$, γ_i "represents the serial number of the sub-image which contains the pixel corresponding to the coordinate $\mid v_1\rangle \mid v_2\rangle ... \mid v_k\rangle$". Simply — index of a sub-image.

The idea of image cropping index allows to retrieve a target sub-image (segmentation) from a quantum system. Additionally, a single qubit is a cheap way of color representation. Li et al. described image encryption based on normal arbitrary superposition state (Li et al. 2019). Based on geometric transformations of multidimensional color images based on normal arbitrary superposition state authors provide such transformations as two-point swapping, flip (including local), orthogonal rotation, and translation (Fan et al. 2016). Zhou and Sun proposed multidimensional color images similarity comparison for QNASS encoded images (Zhou and Sun 2015).

2.3 Pure discrete representation

Representation algorithms of this chapter utilize only discrete amplitude encoding for both pixel intensity and coordinates. Methods described here utilize the multicontrol CX-gate as in Fig. 4.

2.3.1 NEQR

Authors (Zhang et al. 2013) suggest to use full intensity binary expansion for image encoding. The most powerful thing of this explicitly encoded approach is the possibility to read intensity determinedly. The image with the intensity range 2^q (where q equals 8 in case of 256 intensity levels) is encoded in the following way:

$$| I\rangle = \frac{1}{2^n} \sum_{Y=0}^{2^n-1} \sum_{X=0}^{2^n-1} \bigotimes_{i=0}^{q-1} \mid C_{YX}^i\rangle \mid YX\rangle \tag{10}$$

where $\mid C_{YX}^i\rangle$ and $\mid YX\rangle$ are intensity and coordinate expansions respectively. The same encoding principle authors of INCQI show in paper (Su et al. 2021). Paper (Caraiman and Manta 2012) describes the similar approach. The former paper describes the major drawbacks of this approach. Firstly, an appropriate number of trials defines the success of image decoding. The more pixels image contains, more trials the decoding procedure needs. Secondly, multicontrol gates perform as deep sub-circuits with additional gates. Each multicontrol gate expands into exponentially many real-QPU primitives. As a result, the encoding is a time-costly process. Finally, real quantum devices limit the encoding process in terms of number of possible gates.

Figure 2e represents an example of the image encoded with NEQR. The algorithm code is available in the repository.

Apart from determinism, the NEQR has several advantages. The paper says about "partial color operations and statistical color operations" (Zhang et al. 2013). The authors of the described paper split all possible image operations into 3 groups:

- Complete Intensity Operations (CC): changes pixel's intensity in a whole image or its area.
- Partial Intensity Operations (PC): changes intensity of pixels in the certain gray-scaled range.
- Color Statistical Operation (CS): computes intensity statistics.

Authors extended approach to the log-polar images in QUALPI (Zhang et al. 2013) (Fig. 2f shows the encoding example). Additionally, such comprehensive processing as complement intensity transformation and upscaling are also described in the book (Yan and Venegas-Andraca 2020).

Next, strong point of the NEQR is a more efficient circuit compression algorithm. The Espresso Boolean expressions compression (Brayton et al. 1984) is a base for this algorithm. While FRQI algorithm compression ratio is 50% of utilized gates, NEQR allows to reduce the number of gates by 75%.

The negative side appears from the determinant approach. Each intensity expansion leads to utilizing as much qubits as the length of the expansion. Thus, the quantum circuit depth increases proportionally to the image intensity resolution. However, image size increases the

Fig. 4 Multicontrol CX gate. Gate consists of 3 control qubits that apply NOT operation on the last one — target — qubit

number of utilized qubits only logarithmically. Next point is that authors do not describe the experimental platform. Because of this, Mastriani (Mastriani 2020) called NEQR "almost a gedankenexperiment". The paper also tells about Classical-to-Quantum interface using for QPU data loading and why NEQR does not follow it.

As a result, NEQR is useful for reliable intensity representation, which supports large images and comprehensive processing. The approach is less applicable for data with high intensity resolution. The qubit entanglement is the pivotal problem of the encoding. This kills the state orthogonality and prevents the one-to-one pixel intensity measurement. However, this encoding approach is bountiful in terms of processing techniques. For instance, identification of desired pixels in an image using Grover's quantum search algorithm (Iqbal and Singh 2021), edge extraction based on Laplacian operator (Fan et al. 2019a), scaling (Zhou et al. 2020), least squares filtering (Wang et al. 2020), morphological gradient (Yang et al. 2018), edge extraction based on classical Sobel operator (Fan et al. 2019b), quantum image histogram (Heidari et al. 2019), edge extraction based on improved Prewitt operator (Zhou et al. 2019), midpoint filter (Ali et al. 2020) dual-threshold quantum image segmentation (Yuan et al. 2020), steganography based on least significant bit (Zhou et al. 2018), erosion and dilation (Li et al. 2019). Finally, the same encoding method is used for LSB-Based quantum audio watermarking (Nejad et al. 2019).

2.3.2 GQIR

The authors (Jiang et al. 2015) refer to the NEQR approach (Section 2.3.1) and suggest an approach to represent nonsquare images. Figure 5 represents the possible nonsquare image with binary intensity expansions `00000000`, `10000000`, and `11111111` respectively for each pixel.

As far as 3 qubits are able to represent up to 4×2 images, therefore 5 states out of 8 are redundant. To keep measured image shape the same as input's, the authors do not encode pixels without intensity value and leave them to have black color with 0 qubit amplitude. This advantage allows to represent images of an arbitrary shape.

The authors suggest image upscaling based on the nearest-neighbor method. In addition, Zhu et al. provided

	00	01	10	11
0	0	128	255	
1				

Fig. 5 Non-square image, empty cells are expanding to powers of 2

encryption scheme (Zhu et al. 2021), Zhou and Wan implemented image scaling based on bilinear interpolation (Zhou and Wan 2021), Zhang et al. extended approach to floating-point quantum representation and proposed two rows interchanging and swap operations (Zhang et al. 2020). We implemented GQIR representation method in our repository.

2.3.3 QRMW

The authors (Şahin and Yilmaz 2018) provide the representation approach for multichannel images. Each channel corresponds to a specific wavelength. QRMW allows "to encode the color values corresponding to the respective wavelength channel of the pixels in the image".

The equation below defines the intensity of each pixel located in the x, y, λ coordinates (where λ represents wavelength channel index):

$$\begin{aligned} &f(\lambda, y, x) = c^0_{\lambda_{yx}}, c^1_{\lambda_{yx}}, ..., c^{q-2}_{\lambda_{yx}}, c^{q-1}_{\lambda_{yx}}, \\ &f(\lambda, y, x) \in [0, 2^q - 1], \quad c^k_{\lambda_{yx}} \in [0, 1], \end{aligned} \tag{11}$$

where $2^q - 1$ is the maximum amplitude of any wavelength. Then, the QRMW image representation is the following:

$$|I\rangle = \frac{1}{\sqrt{2^{b+n+m}}} \sum_{\lambda=0}^{2^b-1} \sum_{y=0}^{2^n-1} \sum_{x=0}^{2^m-1} |f(\lambda, y, x)\rangle \otimes |\lambda\rangle \otimes |yx\rangle, \tag{12}$$

where b defines the number of channels. As a result, the method contains the extended realization of NEQR (Section 2.3.1). In addition, the authors describe image compression, complete and partial color operations, and position operations. The same authors presented the edge detection algorithm (Şahin and Yilmaz 2021) and extended their encoding approach to the multichannel audio representation (Şahin and Yilmaz 2019).

2.3.4 BRQI

The authors (Li et al. 2018) suggest to split image into n bitplanes where n is a resolution of the pixel intensity. Encoding proceeds through availability of the current bitplane in the pixel with current coordinates.

Suppose an example of the gray-scaled 2×2 image with the following pixel intensities: $\{0, 125, 200, 255\}$. The binary expansion for pixel-wise intensity is the following: `00000000`, `01111101`, `11001000`, `11111111`. Taking bits from each expansion, one can receive 8 bitplanes as in Fig. 6.

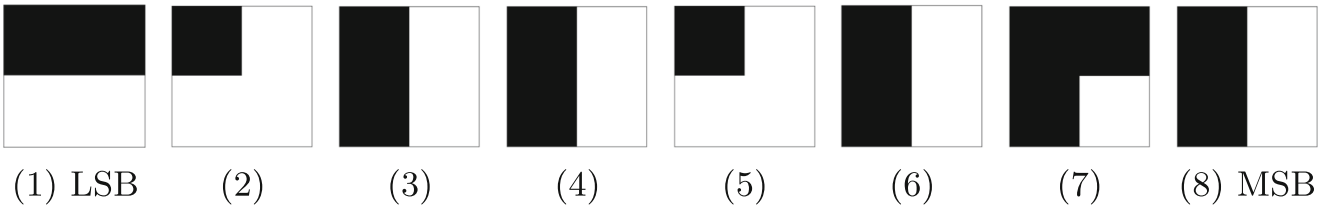

Fig. 6 Bitplane image representation, each letter corresponds to the number of bitplane. The first and the last bits for each bitplane have special names "the least significant bit" (LSB) and "the most significant bit" (MSB) respectively

This paper was inspired by general NEQR approach and defines j^{th} bitplane as follows:

$$| \Psi^j \rangle = \frac{1}{\sqrt{2^n}} \sum_{x=0}^{2^{n-k}-1} \sum_{y=0}^{2^k-1} | g(x,y) \rangle | x \rangle | y \rangle \tag{13}$$

where j denotes the bitplane index ($j = 0, ..., 7$) and $g(x, y) \in \{0, 1\}$ shows presence or absence of a bit in j^{th} bitplane. As a result, the qubit scheme consists of X-, Y-coordinate qubits, bitplane qubits and 1 target qubit, showing availability of the bitplane's current bit. The encoding method is implemented in our repository.

BRQI supports processing operations: bitplane interchange, translation and intensity operation. Heidari et al. proposed selective encryption for the BRQI encoded information (Heidari et al. 2019). Recently, Khorrampanah et al. proposed RGB images encryption (Khorrampanah et al. 2022). The work of Mastriani (2015) deserves special attention, as it describes Quantum Boolean (QuBo) image denoising based on image bitplane splitting. The same paper explains the Classical-to-quantum (C2QI) and Quantum-to-classical interfaces (Q2CI). Later Mastriani proves (Mastriani 2017) reliability of the bitplane splitting approach in terms of C2QI and Q2CI.

To conclude, the BRQI is a promising method in terms of image representation and processing. At the same time, the technique is built upon the NEQR; thus, the number of qubit remains in dependence on the intensity resolution.

2.3.5 QIIR

Indexed images consist of 2 tables: combination of the channel values (first table) and pointers to the palette matrix (second table). An example of such an image is in Fig. 7. Authors (Wang et al. 2020) encode both image's tables ($| Q_{Data} \rangle$ and $| Q_{Map} \rangle$) using NEQR.

Quantum data matrix Inorder to encode $2^n \times 2^n$ Q_{Data} matrix, authors apply NEQR (Section 2.3.1) approach. If (Y, X) is a cell location, I_{YX} is a cell value, then expression is the following:

$$| Q_{Data} \rangle = \frac{1}{2^n} \sum_{Y=0}^{2^n-1} \sum_{X=0}^{2^n-1} | I_{YX} \rangle \otimes | YX \rangle \tag{14}$$

Quantum palette matrix The authors use the same NEQR (Section 2.3.1) approach to encode the color palette. In case of RGB encoding 24 qubits are reserved: 8 for each color. Following equation describes the pallete matrix encoding.

$$| Q_{Map} \rangle = \frac{1}{\sqrt{2^q}} \sum_{j=0}^{2^q-1} | C_j \rangle \otimes | j \rangle \tag{15}$$

Authors provide several processing techniques such as R_y rotation on 90°, cyclic shift, color inversion, color replacement, color look-up, steganography. Besides the authors' suggested processing techniques, no other images handling procedures exist from the best of our knowledge.

The number of utilized qubits is a major disadvantage of the method, as the data literally consist of 2 images.

2.4 Phase representation: FTQR

Grigoryan and Aganyan offer phase-based image encoding (Grigoryan and Agaian 2020).

$$| \breve{f} \rangle = \frac{1}{\sqrt{N}} \sum_{k=0}^{N-1} e^{i\alpha f_k} | k \rangle \tag{16}$$

where $\alpha = 2\pi/1024$. The term $e^{i\alpha f_k} | k \rangle$ allows to map classical intensity values $(0, 255)$ into imaginary plane $(x + i \cdot y)$. Here f_k is in input signal in the coordinate k which expands to x and y. In this way the representation is following:

$$| \breve{f} \rangle = \frac{1}{\sqrt{MN}} \sum_{m=0}^{M-1} \sum_{n=0}^{N-1} e^{i\alpha f_{n,m}} | n, m \rangle \tag{17}$$

Authors do not provide any processing techniques but extend the approach up to multidimensional images. The

Fig. 7 QIIR image representation

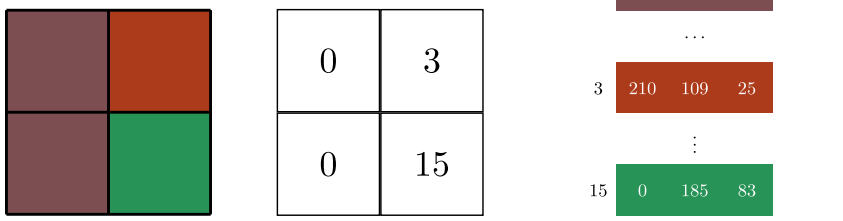

(a) real image (b) Quantum Data Matrix (c) Quantum Palette Matrix

image representation did not take share in the processing techniques research due to its novelty from our opinion. The method is purely phase based, and for measurement it needs phase-to-amplitude transformation. This fact implies additional computation resources.

3 Discussion and conclusion

We reviewed 14 methods of image encoding and propose to categorize them according to classification in Fig. 1. Most of them have the common specific disadvantage, which comes from the quantum computing nature: it is impossible to measure all the pixels in a single trial. For continuous methods, the intensity estimation precision depends on the number of trials. Discrete methods allow to derive information only about 1 pixel from 1 shot. Figure 8 represents the comparison of three metrics for the selected algorithms implemented in our repository: circuit depth, qubit number, and quantum volume.

Tables 1, 2, 3 with columns representing image side size show the same metrics.

We observed that majority of techniques utilize a similar number of qubits; however, the circuit depth shows the highest values for continuous and phase representations and the lowest for the Qubit Lattice approach. The continuous and phase representations are so heavy in depth that we could not execute circuits for images bigger than 32×32. Moreover, for all approaches, we could not succeed in real IBM-Washington (1999) and IonQ (2021) QPU simulation where depth reaches 10^5 for the images of size 4×4 and 8×8 for each machine respectively. This happened because of the multicontrolled rotation gate, which is a base for all continuous and phase methods, is itself expensive for implementation. Following that, it is computationally expensive to simulate high resolution images encoding, especially for continuous and approaches. Additionally, we did not succeed to measure FTQR, and as a result, we were unable to check whether representation works in the full encoding-decoding pipeline correctly. However, FTQR shows the minimum growth of utilized qubits and quantum volume numbers. Considering the number of qubits, Qubit Lattice is the most inappropriate representation algorithm even for IBM-Washington, as qubits can represent at most 8×8 images. Discrete representations stand in between; therefore, they are the most promising group of image representation algorithms.

Each method has its own features. For example, some authors constructed their methods to encode a specific type of image (log-polar, multi-wavelength, indexed).

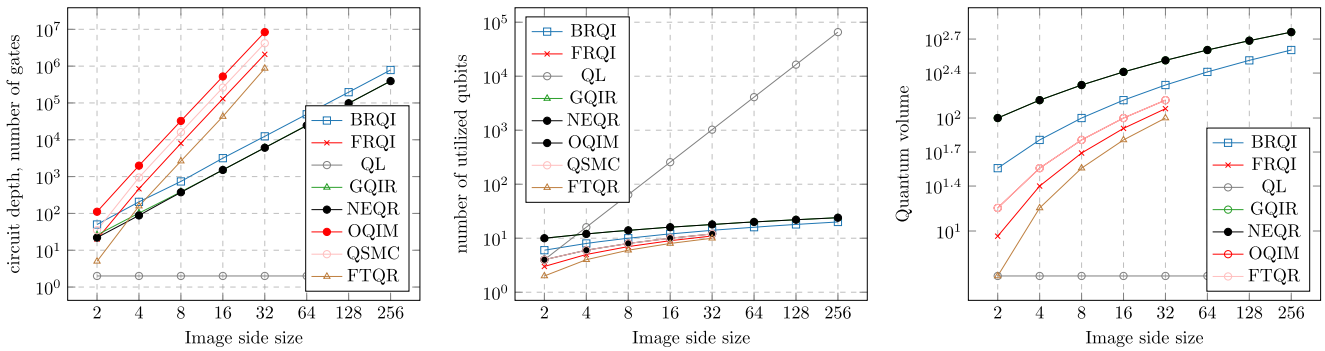

(a) Circuit depth (b) Qubits number (c) Quantum volume

Fig. 8 Metrics

Other authors made an accent on the representation way (based on bitplanes, Fourier transform, order-encoding). While some authors describe their approach in terms of quantum state normality (NAQSS), others operated on color and coordinate differentiation (QSMC and QSNC). This fact might explain the huge number of processing types for the NEQR (Section 2.3.1) and FRQI (Section 2.1.2) representations. Both of them are general, intuitive and appear as main representative for the discrete and continuous groups respectively. Still, NEQR "could perform the complex and elaborate color operation more conveniently than FRQI" (Anand et al. 2022) due to obvious both coordinate and pixel intensity encoding.

The image processing techniques significantly impact image representations. The majority of the discussed methods come with processing algorithms. And yet, the overall stack of available processing is not full. Such comprehensive tools as segmentation, feature extraction, machine learning, recognition keep poor and imperfect review. The survey (Cai et al. 2018) also points to the lack of experience especially on physical equipment. Mastriani (Mastriani 2020) mentions that none of the developed approaches — apart from QuBo — follow the QPU interface conditions. At the same time, research in these branches actively move these topics forward. For instance, authors (Ruan et al. 2021) claims that quantum machine learning and processing of multidimensional data is promising. Thus, opinion about quantum image processing as a "quantum hoax" (Ruan et al. 2021) seems like a matter of time.

We assign our next work to the problems of the image processing in the perspective of machine learning applications. Convolutions, pooling, statistics calculation, and multi-image processing are in the scope of the future work. We are also inspired for further research of the image representation algorithms.

Appendix. Metrics tables

Table 1 Circuit depth

Image encoding	2	4	8	16	32	64	128	256
BRQI	50	206	738	3164	12400	49218	195902	784866
FRQI	467	8003	130307	2094083	–	–	–	–
QL	2	2	2	2	2	2	2	2
GQIR	26	102	389	1491	6180	24511	98014	392236
NEQR	22	88	375	1513	6075	24410	97923	392281
OQIM	111	1983	32511	523263	8382466	–	–	–
QSMC	35	943	16063	260863	4189183	–	–	–
FTQR	5	158	2635	42813	869016	–	–	–

Table 2 Number of utilized qubits

Image encoding	2	4	8	16	32	64	128	256
BRQI	6	8	10	12	14	16	18	20
FRQI	3	5	7	9	11	–	–	–
QL	4	16	64	256	1024	4096	16384	65536
GQIR	10	12	14	16	18	20	22	24
NEQR	10	12	14	16	18	20	22	24
OQIM	4	6	8	10	12	–	–	–
QSMC	4	6	8	10	12	–	–	–
FTQR	4	6	8	10	–	–	–	–

Table 3 Quantum volume

Image encoding	2	4	8	16	32	64	128	256
BRQI	36	64	100	144	196	256	324	400
FRQI	9	25	49	81	121			
QL	4	4	4	4	4	4	4	4
GQIR	100	144	196	256	324	400	484	576
NEQR	100	144	196	256	324	400	484	576
OQIM	16	36	64	100	144	–	–	–
QSMC	16	36	64	100	144	–	–	–
FTQR	4	16	36	64	100	–	–	–

Author contribution Marina Lisnichenko had the idea for the article, performed the literature search and data analysis. Stanislav Protasov critically revised the work.

Data availability Data sharing not applicable to this article as no datasets were generated or analysed during the current study.

Code availability The python code is available in the GitHub repository https://github.com/UralmashFox/QPI.

Declarations

Competing interests The authors declare no competing interests.

References

Ali AE, Abdel-Galil H, Mohamed S (2020) Quantum image mid-point filter. Quantum Inf Process 19(8):1–23. https://doi.org/10.1007/s11128-020-02738-x

Anand A, Lyu M, Baweja PS, Patil V (2022) Quantum image processing. arXiv:2203.01831, https://doi.org/10.48550

Brayton RK, Hachtel GD, McMullen C, Sangiovanni-Vincentelli A (1984) Logic minimization algorithms for VLSI synthesis

Cai Y, Lu X, Jiang N (2018) A survey on quantum image processing. Chin J Electron 27(4):718–727

Caraiman S, Manta V (2012) Image processing using quantum computing. In: 2012 16th International conference on system theory, control and computing (ICSTCC). IEEE, pp 1–6

Cong I, Choi S, Lukin MD (2019) Quantum convolutional neural networks. Nat Phys 15(12):1273–1278. https://doi.org/10.1038/s41567-019-0648-8

Ding M, Huang T-Z, Ji T-Y, Zhao X-L, Yang J-H (2019) Low-rank tensor completion using matrix factorization based on tensor train rank and total variation. J Sci Comput 81(2):941–964. https://doi.org/10.1007/s10915-019-01044-8

Fan P, Zhou R-G, Hu WW, Jing N (2019) Quantum image edge extraction based on laplacian operator and zero-cross method. Quantum Inf Process 18(1):1–23. https://doi.org/10.1007/s11128-018-2129-x

Fan P, Zhou R-G, Hu W, Jing N (2019) Quantum image edge extraction based on classical sobel operator for neqr. Quantum Inf Process 18(1):1–23. https://doi.org/10.1007/s11128-018-2131-3

Fan P, Zhou R-G, Jing N, Li H-S (2016) Geometric transformations of multidimensional color images based on nass. Inf Sci 340:191–208

Farina T (2021) Creating hybrid images using a quantum computer. PhD thesis, UNION COLLEGE

Grigoryan AM, Agaian SS (2020) New look on quantum representation of images: fourier transform representation. Quantum Inf Process 19(5):1–26. https://doi.org/10.1007/s11128-020-02643-3

Grover LK (1997) Quantum computers can search arbitrarily large databases by a single query. Phys Rev Lett 79(23):4709

Guanlei X, Xiaogang X, Xun W, Xiaotong W (2020) A novel quantum image parallel searching algorithm. Optik 209:164565. https://doi.org/10.1016/j.ijleo.2020.164565

Heidari S, Abutalib M, Alkhambashi M, Farouk A, Naseri M (2019) A new general model for quantum image histogram (qih). Quantum Inf Process 18(6):1–20. https://doi.org/10.1007/s11128-019-2295-5

Heidari S, Naseri M, Nagata K (2019) Quantum selective encryption for medical images. Int J Theor Phys 58(11):3908–3926. https://doi.org/10.1007/s10773-019-04258-6

Hu W-W, Zhou R-G, Luo J, Jiang S-X, Luo G-F (2020) Quantum image encryption algorithm based on arnold scrambling and wavelet transforms. Quantum Inf Process 19(3):1–29. https://doi.org/10.1007/s11128-020-2579-9

IBM-Washington (1999) Machine details. https://quantum-computing.ibm.com/services?services=systems&order=qubits=qubits%%20DESC&view=table&system=ibmwashington

IonQ (2021) Best practices for using IonQ hardware: https://ionq.com/best-practices

Iqbal B, Singh H (2021) Identification of desired pixels in an image using grover's quantum search algorithm. arXiv:2107.03053, https://doi.org/10.48550

Jiang N, Wang J, Mu Y (2015) Quantum image scaling up based on nearest-neighbor interpolation with integer scaling ratio. Quantum Inf Process 14(11):4001–4026. https://doi.org/10.1007/s11128-015-1099-5

Khorrampanah M, Houshmand M, Lotfi Heravi MM (2022) New method to encrypt rgb images using quantum computing. Opt Quant Electron 54(4):1–16. https://doi.org/10.1007/s11082-022-03581-3

Latorre JI (2005) Image compression and entanglement. arXiv:quant-ph/0510031, https://doi.org/10.48550

Le PQ, Dong F, Hirota K (2011) A flexible representation of quantum images for polynomial preparation, image compression, and processing operations. Quantum Inf Process 10(1):63–84. https://doi.org/10.1007/s11128-010-0177-y

Leprince-Ringuet D (2021) Daphne leprince-ringuet: quantum computing is at an early stage. But investors are already getting excited. https://www.zdnet.com/article/quantum-computing-is-at-an-early-stage-but- investors-are-already-getting-excited/

Li H-S, Chen X, Xia H, Liang Y, Zhou Z (2018) A quantum image representation based on bitplanes. IEEE Access 6:62396–62404

Li H-S, Li C, Chen X, Xia H (2019) Quantum image encryption based on phase-shift transform and quantum haar wavelet packet transform. Modern Phys Lett A 34(26):1950214. https://doi.org/10.1142/S0217732319502146

Li H-S, Qingxin Z, Lan S, Shen C-Y, Zhou R, Mo J (2013) Image storage, retrieval, compression and segmentation in a quantum system. Quantum Inf Process 12(6):2269–2290. https://doi.org/10.1007/s11128-012-0521-5

Li P, Shi T, Lu A, Wang B (2019) Quantum circuit design for several morphological image processing methods. Quantum Inf Process 18(12):1–35. https://doi.org/10.1007/s11128-019-2479-z

Li H-S, Zhu Q, Zhou R-G, Song L, Yang X-J (2014) Multi-dimensional color image storage and retrieval for a normal arbitrary quantum superposition state. Quantum Inf Process 13(4):991–1011.

Liu X, Xiao D (2019) Multimodality image fusion based on quantum wavelet transform and sum-modified-laplacian rule. Int J Theor Phys 58(3):734–744. https://doi.org/10.1007/s10773-018-3971-4

Ma H, He Z, Xu P, Dong Y, Fan X (2020) A quantum richardson–lucy image restoration algorithm based on controlled rotation operation and hamiltonian evolution. Quantum Inf Process 19(8):1–14. https://doi.org/10.1007/s11128-020-02723-4

Ma G, Li H, Zhao J (2021) Quantum radon transform and its application. arXiv:2107.05524

Mastriani M (2015) Quantum boolean image denoising. Quantum Inf Process 14(5):1647–1673. https://doi.org/10.1007/s11128-014-0881-0

Mastriani M (2017) Quantum image processing? Quantum Inf Process 16(1):1–42. https://doi.org/10.1007/s11128-014-0881-0

Mastriani M (2020) Quantum image processing: the pros and cons of the techniques for the internal representation of the image. a reply to: a comment on quantum image processing? Quantum Inf Process 19(5):1–17

Nejad MY, Mosleh M, Heikalabad SR (2019) An lsb-based quantum audio watermarking using msb as arbiter. Int J Theor Phys 58(11):3828–3851. https://doi.org/10.1007/s10773-019-04251-z

Oh S, Choi J, Kim J (2020) A tutorial on quantum convolutional neural networks (qcnn). In: 2020 International conference on information and communication technology convergence (ICTC). IEEE, pp 236–239

Ruan Y, Xue X, Shen Y (2021) Quantum image processing: opportunities and challenges. Math Probl Eng, vol 2021. https://doi.org/10.1155/2021/6671613

Şahin E, Yilmaz I (2018) Qrmw: quantum representation of multi wavelength images. Turkish J Electr Eng Comput Sci 26(2):768–779. https://doi.org/10.3906/elk-1705-396

Şahin E., Yilmaz İ. (2019) Qrma: quantum representation of multi-channel audio. Quantum Inf Process 18(7):1–30. https://doi.org/10.1007/s11128-019-2317-3

Şahin E, Yilmaz İ. (2021) A quantum edge detection algorithm for quantum multi-wavelength images. Int J Quantum Inf 19(03):2150017. https://doi.org/10.1142/S0219749921500179

Sanchez M, Sun G-H, Dong S-H (2019) Correlation property of multipartite quantum image. Int J Theor Phys 58(11):3773–3796. https://doi.org/10.1007/s10773-019-04247-9

Shende VV, Bullock SS, Markov IL (2006) Synthesis of quantum-logic circuits. IEEE Trans Comput-Aided Design Integrated Circuits Syst 25(6):1000–1010. https://doi.org/10.1145/1120725.1120847

Su J, Guo X, Liu C, Lu S, Li L (2021) An improved novel quantum image representation and its experimental test on ibm quantum

experience. Sci Reports 11(1):1–13. https://doi.org/10.1038/s41598-021-93471-7
Sun B, Iliyasu AM, Yan F, Sanchez JAG, Dong F, Al-Asmari AK, Hirota K (2014) Multi-channel information operations on quantum images. J Adv Computat Intell Intell Inf 18(2):140–149
Sun B, Le PQ, Iliyasu AM, Yan F, Garcia JA, Dong F, Hirota K (2011) A multi-channel representation for images on quantum computers using the rgbα color space. In: 2011 IEEE 7th international symposium on intelligent signal processing. IEEE, pp 1–6. https://doi.org/10.1109/WISP.2011.6051718
Tariq Jamal A, Abdel-Khalek S, Ben Ishak A (2021) Multilevel segmentation of medical images in the framework of quantum and classical techniques. Multimed Tools Appl:1–14. https://doi.org/10.1007/s11042-020-10235-7
Thenmozhi S, BalaSubramanya K, Shrinivas S, Joshi SKD, Vikas B (2021) Information hiding using quantum image processing state of art review. Inventive Computat Inf Technol, pp 235–245. https://doi.org/10.1007/978-981-33-4305-4_18
Venegas-Andraca SE, Bose S (2003) Storing, processing, and retrieving an image using quantum mechanics. In: Quantum information and computation, vol 5105, pp 137–147. https://doi.org/10.1117/12.485960. International society for optics and photonics
Wang B, Hao M-Q, Li P-C, Liu Z-B (2020) Quantum representation of indexed images and its applications. Int J Theoretical Phys 59(2):374–402. https://doi.org/10.1007/s10773-019-04331-0
Wang S, Xu P, Song R, Li P, Ma H (2020) Development of high performance quantum image algorithm on constrained least squares filtering computation. Entropy 22(11):1207. https://doi.org/10.3390/e22111207
Xu G, Xu X, Wang X, Wang X (2019) Order-encoded quantum image model and parallel histogram specification. Quantum Inf Process 18(11):1–26. https://doi.org/10.1007/s11128-019-2463-7
Yan F, Iliyasu AM, Jiao S, Yang H (2018) Audio-visual synchronisation in quantum movies. In: 2018 IEEE 5th international congress on information science and technology (CiSt). IEEE, pp 274–278
Yan F, Jiao S, Iliyasu AM, Jiang Z (2018) Chromatic framework for quantum movies and applications in creating montages. Frontiers Comput Sci 12(4):736–748. https://doi.org/10.1007/s11704-018-7070-8
Yan F, Venegas-Andraca SE (2020) Quantum image processing
Yang C-HH, Qi J, Chen SY-C, Chen P-Y, Siniscalchi SM, Ma X, Lee C-H (2021) Decentralizing feature extraction with quantum convolutional neural network for automatic speech recognition. In: ICASSP 2021-2021 IEEE international conference on acoustics, speech and signal processing (ICASSP). IEEE, pp 6523–6527
Yang J, Zhu Y, Li K, Yang J, Hou C (2018) Tensor completion from structurally-missing entries by low-tt-rankness and fiber-wise sparsity. IEEE J Select Topics Signal Process 12(6):1420–1434. https://doi.org/10.1109/JSTSP.2018.2873990
Yuan S, Mao X, Xue Y, Chen L, Xiong Q, Compare A (2014) Sqr: a simple quantum representation of infrared images. Quantum Inf Process 13(6):1353–1379. https://doi.org/10.1007/s11128-014-0733-y
Yuan S, Wen C, Hang B, Gong Y (2020) The dual-threshold quantum image segmentation algorithm and its simulation. Quantum Inf Process 19(12):1–21. https://doi.org/10.1007/s11128-020-02932-x
Zhang Y, Lu K, Gao Y, Wang M (2013) Neqr: a novel enhanced quantum representation of digital images. Quantum Inf Process 12(8):2833–2860. https://doi.org/10.1007/s11128-013-0567-z
Zhang Y, Lu K, Gao Y, Xu K (2013) A novel quantum representation for log-polar images. Quantum Inf Process 12(9):3103–3126. https://doi.org/10.1007/s11128-013-0587-8
Zhang R, Xu M, Lu D (2020) A generalized floating-point quantum representation of 2-d data and their applications. Quantum Inf Process 19(11):1–20. https://doi.org/10.1007/s11128-020-02895-z
Zhou R-G, Cheng Y, Qi X, Yu H, Jiang N (2020) Asymmetric scaling scheme over the two dimensions of a quantum image. Quantum Inf Process 19(9):1–20. https://doi.org/10.1007/s11128-020-02837-9
Zhou R-G, Luo J, Liu X, Zhu C, Wei L, Zhang X (2018) A novel quantum image steganography scheme based on lsb. Int J Theor Phys 57(6):1848–1863. https://doi.org/10.1007/s10773-018-3710-x
Zhou R-G, Sun Y-J (2015) Quantum multidimensional color images similarity comparison. Quantum Inf Process 14(5):1605–1624. https://doi.org/10.1007/s11128-014-0849-0
Zhou R-G, Tan C, Ian H (2017) Global and local translation designs of quantum image based on frqi. Int J Theor Phys 56(4):1382–1398. https://doi.org/10.1007/s10773-017-3279-9
Zhou R-G, Wan C (2021) Quantum image scaling based on bilinear interpolation with decimals scaling ratio. Int J Theor Phys 60(6):2115–2144. https://doi.org/10.1007/s10773-021-04829-6
Zhou R-G, Yu H, Cheng Y, Li F-X (2019) Quantum image edge extraction based on improved prewitt operator. Quantum Inf Process 18(9):1–24. https://doi.org/10.1007/s11128-019-2376-5
Zhu H-H, Chen X-B, Yang Y-X (2021) A multimode quantum image representation and its encryption scheme. Quantum Inf Process 20(9):1–21. https://doi.org/10.1007/s11128-021-03255-1

Marina Lisnichenko received the M.S. in robotics from Innopolis University in 2021. She is currently pursuing the PhD degree with the Machine Learning and Knowledge Representation lab, Innopolis University. Her research interests include quantum information processing, quantum circuit compression, geographic information processing.

Stanislav Protasov received the PhD degree in the computer science from Voronezh State University in 2013. He is currently an Associate Professor with Innopolis University. His research interests include applied machine learning, information retrieval, applications of quantum computing, quantum state preparation.